Enhanced spin coherence via mesoscopic confinement during acoustically induced transport

New Journal of Physics
The open-access journal for physics

Enhanced spin coherence via mesoscopic confinement during acoustically induced transport

J A H Stotz[1,2,3], **R Hey**[1], **P V Santos**[1] **and K H Ploog**[1]

[1] Paul-Drude-Institut für Festkörperelektronik, Hausvogteiplatz 5–7, 10117 Berlin, Germany

[2] Department of Physics, Engineering Physics and Astronomy, Queen's University, Kingston, ON K7L 3N6, Canada

E-mail: jstotz@physics.queensu.ca

New Journal of Physics **10** (2008) 093013 (10pp)
Received 10 July 2008
Published 12 September 2008
Online at http://www.njp.org/
doi:10.1088/1367-2630/10/9/093013

Abstract. Long coherence lifetimes of electron spins transported using moving potential dots are shown to result from the mesoscopic confinement of the spin vector. The confinement condition to control electron spin dephasing is governed by the relation between the characteristic spin–orbit length of the electron spins and the dimensions of the dot potential, which governs the electron spin coherence lifetime. The spin–orbit length is a sample-dependent parameter determined by the Dresselhaus contribution to the spin–orbit coupling and can be predictably controlled by varying the sample geometry. We further show that the coherence lifetime of the electron spins is independent of the local carrier densities within each potential dot, which suggests the possibility of coherent, long-range transport of single electron spins.

Contents

1. Introduction 2
2. Experiment 3
3. Experimental results and discussion 3
4. Conclusions 8
Acknowledgments 9
References 9

[3] Author to whom any correspondence should be addressed.

1. Introduction

The ability to store and transport quantum excitations is a critical step towards the application of quantum effects to information processing. In particular, the coherent storage and transport of electron spins in spintronic devices based on semiconductor nanostructures can be used to process quantum bits. Understanding and limiting the various spin decoherence mechanisms in semiconductors has become, therefore, an important field of research that has seen considerable effort. The high material quality of GaAs-based semiconductors has reduced extrinsic spin scattering to the point where the primary decoherence mechanism for moving spins results from intrinsic D'yakonov–Perel' (DP) spin dephasing [1]. DP effects typically arise from the random thermal motion of the electron spins in the effective, internal magnetic field $\mathbf{B}_{\text{int}}(\mathbf{k})$ associated with the spin–orbit splitting of the conduction band for electrons with nonzero wavevector $\mathbf{k}$. In the presence of $\mathbf{B}_{\text{int}}(\mathbf{k})$, the coherence of an initially polarized electron spin ensemble is lost as individual spins follow distinct random walks—each with a different set of non-commutative rotations about $\mathbf{B}_{\text{int}}(\mathbf{k})$. DP spin dephasing can be controlled through motional narrowing, whereby rapid momentum scattering times τ_{p} reduce the precession angles during the random walk (and, consequently, increase the spin dephasing time τ_{s}) according to the inverse relationship $\tau_{\text{s}} \sim \tau_{\text{p}}^{-1}$ [1, 2]. This motional narrowing mechanism has been invoked to explain the long spin coherence times in n-type GaAs [3].

A novel process to coherently transport spins relies on the use of mobile potentials with mesoscopic, micron-sized dimensions. In fact, we have recently demonstrated that the effects of DP dephasing can be significantly reduced using mobile confinement potentials induced by coherent acoustic phonons [4]. The phonons, generated in the form of surface acoustic waves (SAWs), create a moving, three-dimensional piezoelectric confinement potential (referred to as dynamic quantum dots (DQDs)) that coherently transports spin-polarized electrons over long distances (on the order of 100 μm). One interesting question, which will be the subject discussed here, regards the mechanisms leading to the reduced DP dephasing. Two possibilities were originally proposed [4]. The first suggests that the spin lifetime enhancements arise from motional narrowing associated with the high local electron density within the DQDs, similar to the effects observed in GaAs quantum wells (QWs) [5, 6]. The second possibility lends itself to the fact that when spins are mesoscopically confined to dimensions smaller than the spin–orbit length λ_{SO}, defined as the ballistic transport distance required for a precession angle of 1 rad around $\mathbf{B}_{\text{int}}(\mathbf{k})$, random spin precession due to thermal motion becomes suppressed, and the DP spin dephasing is limited [2], [7]–[12]. In this case, the coherence enhancement intuitively arises from the motional narrowing associated with the electron scattering on the potential boundaries. The implications of this scenario would prove to be quite dramatic. Confinement from the acoustically induced potential would provide a platform for the transport and manipulation of single bits of spin information given that previous experiments on SAW systems have shown single-electron transistors [13] and the theoretical discussions of SAW-based quantum computing [14, 15].

Here, we unambiguously show that the long spin coherence lengths observed during transport via DQDs result from mesoscopic confinement effects. In fact, spin transport measurements performed by varying the density of optically injected electrons over an order of magnitude demonstrate that the spin coherent transport length, l_{s}, and hence the spin lifetime, is not affected by the local electron concentration. In contrast, l_{s} reduces dramatically when the spin–orbit length becomes comparable with or less than the lateral size of the DQD, L_{DQD}.

We examine this effect through experiments in which λ_{SO}, which is primarily determined by Dresselhaus spin–orbit effects, is varied by changing the thickness of the GaAs QWs and, in particular, show that the experimental results reflect the $l_s \propto (\lambda_{SO})^2$ dependence associated with DP spin dephasing. As a result, motional narrowing effects do not depend on carrier densities, and the ability to control spin coherence during transport down to the single spin level is possible in the SAW system.

2. Experiment

The DQDs are produced by the interference of two SAW beams propagating along the ⟨110⟩ surface directions of a GaAs QW sample [16, 17]. Three single-QW samples with $Al_{0.3}Ga_{0.7}As$ barriers were grown by molecular-beam epitaxy on GaAs (001) semi-insulating substrates. Two were designed with thicknesses of 12 and 20 nm and placed 390 nm below the surface, whereas the third, 30 nm-thick QW was placed 175 nm below the surface. The SAWs are excited by applying a radio-frequency signal to two aluminium split-finger interdigitated transducers deposited on the sample surface using standard optical lithography protocols, and each beam has a linear power density between 2 and 7 W m^{-1}. The SAWs have a wavelength λ_{SAW} of 5.6 μm, corresponding to a frequency $\Omega_{SAW}/2\pi$ of 519 MHz at a sample temperature of 12 K and propagate with a well-defined phase velocity of $v_{SAW} = 2907$ m s^{-1}. The type-II piezoelectric potential generated by the interference of the two plane waves confines and transports the photogenerated electrons and holes within a $120 \times 120\,\mu m^2$ array of DQDs, with the diameter of each dot L_{DQD} being approximately 1 μm. The DQD array propagates along a ⟨100⟩-direction with a velocity $v_{DQD} = \sqrt{2} v_{SAW}$ and has a periodicity $\lambda_{DQD} = \sqrt{2}\lambda_{SAW}$. The measurements were performed at sample temperatures of either 4.2 or 12 K. As has been previously reported, the electron spin coherence is insensitive to temperatures in this range [18].

The coherent spin transport was monitored by microscopic photoluminescence (PL) measurements (cf figure 1). A circularly polarized, 768 nm laser beam was focused onto the sample to photogenerate spin-polarized electrons and holes at a position G. The carrier densities n are estimated by $n = 2\pi P_{ph} e^{-\alpha d_{QW}}/(E_{ph}\Omega_{DQD})$, where P_{ph} is the incident light power, E_{ph} is the photon energy, α is the absorption coefficient in the GaAs QW, d_{QW} is the QW width, and $\Omega_{DQD} = \Omega_{SAW}$ is the DQD frequency. After excitation, the carriers are spatially separated by the piezoelectric potential onto different phases of the DQD lattice and transported along well defined channels. This efficient charge separation by the acoustically induced potential strongly suppresses spin exchange scattering via the Bir–Aronov–Pikus mechanism during transport [19, 20]. While some recombination occurs due to electronic traps in the DQD channel, most luminescence is observed near the edge of a semi-transparent metal strip M that partially screens the piezoelectric potential of the DQDs and allows the electrons and holes to recombine. The degree of circular polarization $\rho_z = (I_R - I_L)/(I_R + I_L)$ of the luminescence near M can then be measured, where I_R and I_L are the right- and left-circular components of the PL, respectively. The dependence of ρ_z on the transport distance is mapped by varying the separation between G and M. Because of the rapid scattering of hole spins in GaAs [21], ρ_z correlates well with the net electron spin population.

3. Experimental results and discussion

Figure 2 shows the spatial dependence of ρ_z for three different electron densities ranging across an order of magnitude (from 15 to 140 electrons per DQD), which correspond to volume

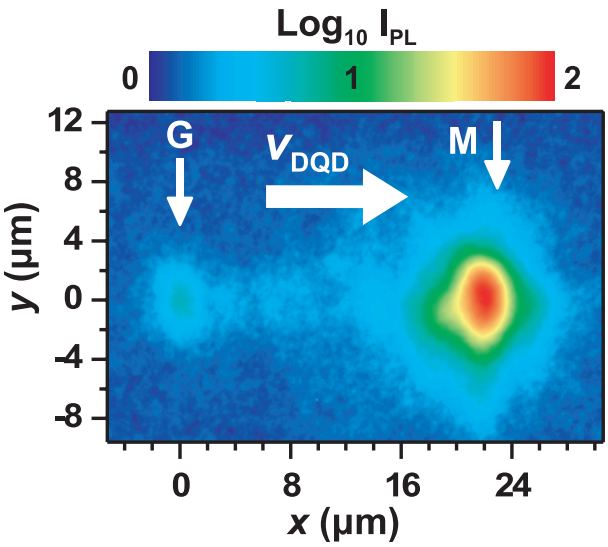

Figure 1. Spatially resolved PL image of carrier transport in a 12 nm QW. Spin-polarized carriers are photogenerated at G and transported to the edge of a semitransparent metal strip M, which induces electron–hole recombination. The circular polarization of the PL maximum near M is used to map the spin transport. The sample temperature was 12 K.

(area) concentrations of approximately 10^{14}–$10^{15}\,\mathrm{cm}^{-3}$ (10^{8}–$10^{9}\,\mathrm{cm}^{-2}$). The measured values of polarization were fitted with a function of the form $\rho_z(x) = \rho_0\, \mathrm{e}^{-x/l_\mathrm{s}} \cos(\Omega_\mathrm{L}^\mathrm{D}(k_\mathrm{DQD})x/v_\mathrm{DQD})$, where ρ_0 represents the initial spin polarization at G, and l_s is the spin coherence length. The oscillations in ρ_z result from the precession of the electron spins around $\mathbf{B}_\mathrm{int}(\mathbf{k}_\mathrm{DQD})$ with a frequency $\Omega_\mathrm{L}^\mathrm{D}$ during transport. The coherent precession observed here occurs in the absence of an external magnetic field and is, for the present sample, primarily related to the $\mathbf{B}_\mathrm{int}(k_\mathrm{DQD})$ associated with the spin–orbit contribution due to the lack of bulk inversion symmetry in the zinc-blende crystal (Dresselhaus term) [22, 23]. Consequently, the Larmor frequency of the electron spin precession can be described by

$$\Omega_\mathrm{L}^\mathrm{D}(k_\mathrm{DQD}) = \frac{\gamma}{\hbar} k_\mathrm{DQD} \langle k_z \rangle^2 = \frac{\gamma}{\hbar} k_\mathrm{DQD} \left(\frac{\pi}{d_\mathrm{eff}}\right)^2, \tag{1}$$

where γ is the spin–orbit parameter, $k_\mathrm{DQD} = m^* v_\mathrm{DQD}/\hbar$ is the average momentum of the electrons within the DQDs, m^* is the electron effective mass, k_z describes the momentum due to the QW confinement, and d_eff is the effective QW thickness including the penetration d_0 of the electron wavefunction into the $Al_{0.3}Ga_{0.7}As$ barrier layer [24]. The latter was calculated using a tight-binding approach yielding a value of $d_0 = 2.1$ nm for each barrier. There is also a contribution to $\Omega_\mathrm{L}^\mathrm{D}(k_\mathrm{DQD})$ from the Bychkov–Rashba (BR) term [25] related to a structural inversion asymmetry induced, for example, by the vertical component of the piezoelectric field, but both are small for the present experimental conditions and will be neglected [23].

For the electron densities presented in figure 2, the spin coherence lengths l_s are comparable and greater than 100 μm. Likewise, the coherence times $T_2^* = l_\mathrm{s}/v_\mathrm{DQD}$ of the electron spin microensemble within each DQD remain essentially unchanged. This is in stark contrast to lifetime measurements on unconfined systems, such as bulk GaAs [3, 26] and GaAs QWs [5, 6],

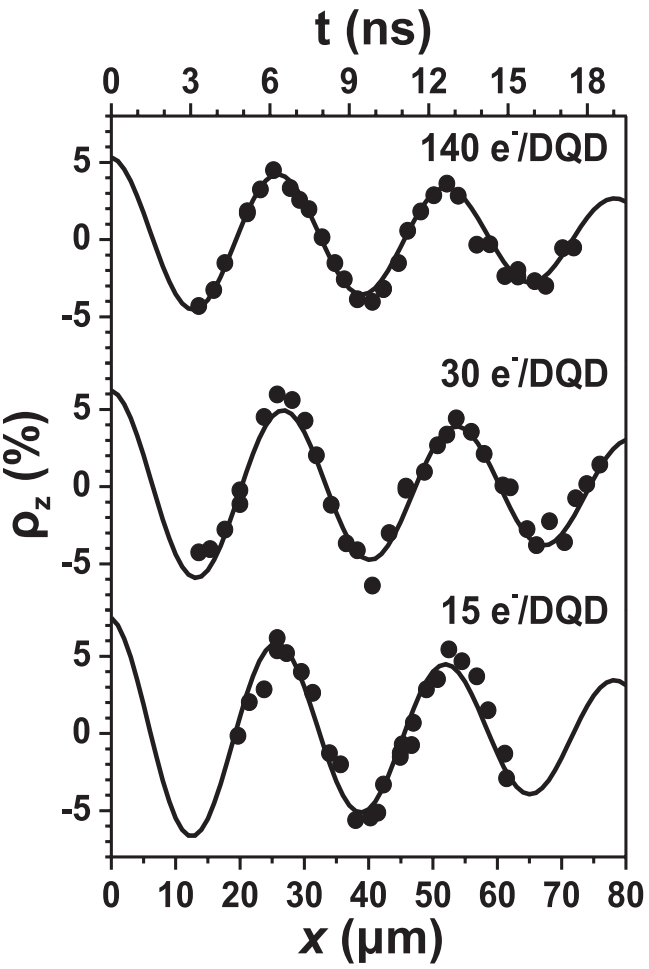

Figure 2. Spatial dependence of ρ_z recorded at varying carrier densities in a 20 nm-thick QW. The symbols and solid lines represent the measured values of ρ_z and the numerical fits, respectively. All curves provide the spin coherence lengths l_s in the range 110 ± 30 μm. The time axis t is determined by $t = x/v_{DQD}$.

where the spin lifetime has been shown to be strongly carrier-dependent. The long spin lifetimes observed during transport by DQDs cannot, therefore, be attributed to motional narrowing resulting from the mechanisms discussed in previous reports [3, 6, 26, 27]. Instead, we attribute motional narrowing effects to the DQD piezoelectric confinement of the electron spins. We argue that the confinement is effective because the size of the DQD L_{DQD} is sufficiently small to prevent large precession angles of individual spins during random thermal motion within the DQDs. The effect of confinement on quantum coherence has been previously studied experimentally [8] as well as theoretically [28], in addition to the discussion of weak localization of electrons in a stationary quantum dot with dimensions smaller than the spin–orbit length λ_{SO} [7, 9].

In the context of the enhanced, long-range transport of quantum states presented here, it is thus anticipated that λ_{SO} has a larger spatial extent than the approximately 1 μm diameter of the DQDs (L_{DQD}). As mentioned above, the spin–orbit length λ_{SO} can be intuitively characterized by the distance it takes a spin to precess 1 radian around $\mathbf{B}_{int}(k)$ [2, 10]. Concerning the

contribution to λ_{SO} due to the Dresselhaus spin–orbit interaction, the temperatures and carrier densities for a QW system relevant to the experiment conditions allow the linear term in **k** to dominate over the cubic term [24]. As a result, the Larmor precession frequency associated with the random motion $\Omega_L^D(k_F)$ is obtained from equation (1) by replacing of k_{DQD} by the Fermi wavevector of the electrons k_F. As discussed above, the spin–orbit contribution to the Larmor precession from the BR-term and from the induced strain are small compared with the Dresselhaus contribution and will be neglected. Consequently, this approximation results in an isotropic λ_{SO} given by

$$\lambda_{SO} = \frac{v_F}{\Omega_L^D(k_F)} = \frac{\hbar^2 (d_{eff})^2}{\pi^2 \gamma m^*}. \tag{2}$$

Interestingly, the Fermi wavevector k_F does not appear in equation (2) demonstrating that λ_{SO} is *independent* of the electron momentum k in this linear approximation. Therefore, we can experimentally extract $\lambda_{SO} = v_{DQD}/\Omega_L^D(k_{DQD})$ directly from the measured precession frequency of the spins.

The Larmor precession frequency of the oscillations shown in figure 2 are quite uniform with a frequency $\Omega_L^D = 0.97\,\mathrm{ns}^{-1}$. This is similar to the value ($1.1\,\mathrm{ns}^{-1}$) that we have previously published for comparable DQD acoustic power densities [4]. The slight difference is accounted for by dissimilarities in the mounting of the sample in the cryostat that may have introduced a slightly different static strain of the sample during cooling to 12 K [29, 30]. Using the value of $\Omega_L^D = 0.97\,\mathrm{ns}^{-1}$, we obtain a spin–orbit length $\lambda_{SO} = 4.2\,\mu\mathrm{m}$ for the 20 nm QW sample, which is expectedly larger than the DQD confinement dimensions L_{DQD} of approximately 1 μm. As a result, the mesoscopic DQD confinement potential does indeed provide the motional narrowing required to maintain the spin coherence of the microensemble within the DQD.

The preceding demonstration of the mesoscopic confinement of the electrons spins now allows us to further explore the relationship between the spin–orbit length, the confinement dimensions and the coherence length. According to equation (1), the Larmor precession frequency of the electron spins, and hence the spin–orbit length, can be varied by changing the thickness of the QW. As discussed by Chang *et al*, changing the relationship between λ_{SO} with respect to the size of the dot will have dramatic effects on spin coherence that are equivalent to changing the size of the confinement potential [11]. To exploit the λ_{SO} dependence, we have performed spin transport measurements on samples with different QW thicknesses. Figure 3 compares ρ_z for the previously discussed 20 nm QW sample with similar samples consisting of single QWs of thicknesses 12 and 30 nm; important parameters from this figure are summarized in table 1. The thinner 12 nm QW shows a dramatic increase in the Larmor precession frequency that is in good agreement with the value expected using equation (1). In fact, using the measured values of $\Omega_L^D(k_{DQD})$ from the 12 and 20 nm QW samples along with the well-defined DQD wavevector k_{DQD}, the spin–orbit parameter γ is calculated to be 17 and 16 eV Å^3, respectively, using equation (1). These are in agreement with our previously determined value of 17 ± 2 eVÅ^3 [23].

In our approximation, electron spins at the Fermi surface will experience the same increase in $\Omega_L^D(k_F)$ as $\Omega_L^D(k_{DQD})$ when the QW thickness is reduced. As shown in table 1, this will result in an inversely proportional modification of the spin–orbit length λ_{SO}. As $\lambda_{SO}(\Omega_L^D)$ is reduced in the 12 nm-thick QW sample, it becomes similar to the spatial dimensions of the DQDs L_{DQD}. As a result, the *effective* confinement of the spins is therefore less than that for the 20 nm QW sample leading to shorter coherence lengths l_s, which is approximately proportional to the square of the

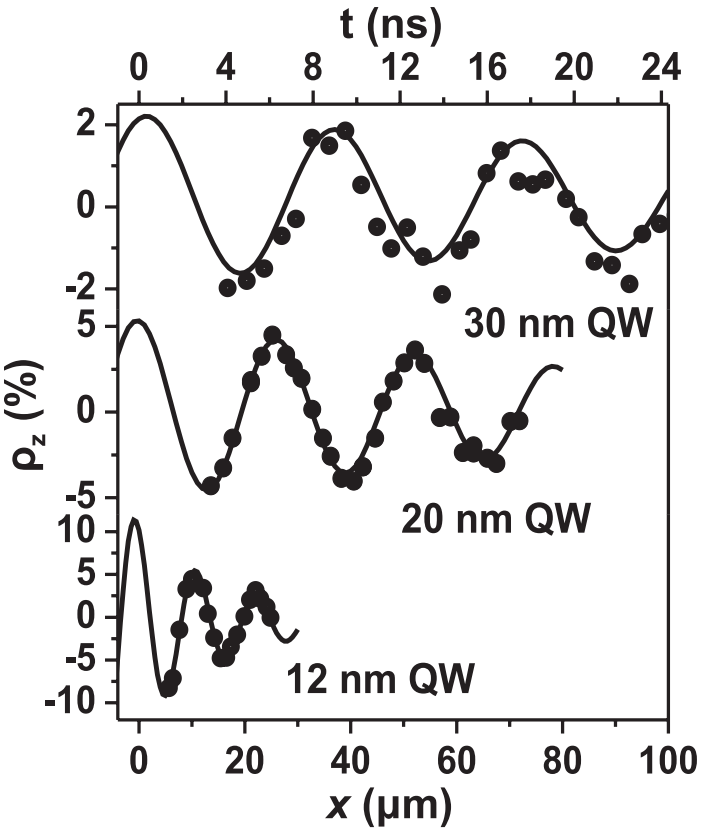

Figure 3. Spatial dependence of ρ_z for QWs with thicknesses of 30, 20 and 12 nm. The symbols and solid lines represent the measured values of ρ_z and the numerical fits, respectively. The time axis t is determined by $t = x/v_{\mathrm{DQD}}$.

Table 1. Spin transport parameters for three different QW samples. The calculated $\Omega_{\mathrm{L}}^{\mathrm{D}}$ uses equation (1) and a value of $\gamma = 17\,\mathrm{eV\AA}^3$ [23]. λ_{SO} was determined using the measured values of $\Omega_{\mathrm{L}}^{\mathrm{D}}$. The coherence lengths l_{s} correspond to the fitted curves in figure 3, and the values in brackets compare the 110 μm coherence length from the 20 nm QW adjusted by the change in the spin–orbit length $(\lambda_{\mathrm{SO}})^2$. Similarly, the final column presents the values $(\lambda_{\mathrm{SO}})^2/l_{\mathrm{s}}$ highlighting the relationship between the spin–orbit length and the coherence length.

QW sample	$\Omega_{\mathrm{L}}^{\mathrm{D}}(k_{\mathrm{DQD}})(\mathrm{ns}^{-1})$ (Meas.)	(Calc.)	λ_{SO} (μm)	l_{s} (μm)	$(\lambda_{\mathrm{SO}})^2/l_{\mathrm{s}}$ (μm)
30 nm	0.73	0.52	5.6	$200(194) \pm 115$	0.16 ± 0.90
20 nm	0.97	1.03	4.2	110 ± 28	0.16 ± 0.04
12 nm	2.26	2.31	1.8	$17(20) \pm 2$	0.19 ± 0.03

spin–orbit length $(\lambda_{\mathrm{SO}})^2$ and is indicative of the DP dephasing becoming dominant in the spin coherence. Monolayer fluctuations in the QW thickness d_{eff} will create additional pathways for spin dephasing, but the 1–2% variations in $\Omega_{\mathrm{L}}^{\mathrm{D}}$ would not be sufficient to account for the dramatic changes observed in the spin coherence length.

For the 30 nm-thick QW sample, the measured Larmor precession frequency is larger than that expected using equation (1). This is attributed to the increasing importance of the strain components to $\mathbf{B}_{\text{int}}(\mathbf{k})$ considering the smaller Dresselhaus term for this QW thickness (cf equation (1)) and that the QW is nearer to the surface than in the other samples—the specifics of which will be discussed in detail in a later publication. Using the experimentally determined $\Omega_{\text{L}}^{\text{D}}$, λ_{SO} is nevertheless determined to be 5.6 μm. This larger spin–orbit length is expected to increase the spin coherence length to 194 μm (given the $(\lambda_{\text{SO}})^2$ proportionality), and the measured $l_{\text{s}} = 200 \pm 115$ μm is consistent with this expectation. The larger error in this measurement is attributed to the fact that the measured transport range is only a small fraction of the long coherence length. However, the work does indicate that increasing the confinement during spin transport in a DQD (via a larger $\lambda_{\text{SO}}/L_{\text{DQD}}$ ratio) will enable longer coherence lengths.

Intuitively, the enhanced electron spin lifetimes result from the ability of the mesoscopic confinement potential to rapidly scatter the electron momentum and prevent a spin from undergoing the large precession angles during its mean free path that cause DP dephasing. Our sample set suggests that the spin coherence length follows a quadratic dependence with respect to the spin–orbit length. The general relation used to describe DP spin dephasing is [1, 2]

$$\tau_{\text{s}} \sim [\Omega_{\text{L}}^{\text{D}}(k_{\text{F}})]^{-2}\tau_{\text{p}}^{-1} \sim (\lambda_{\text{SO}})^2\tau_{\text{p}}^{-1}. \tag{3}$$

Equation (3) reflects our observed quadratic dependence in $\lambda_{\text{SO}}(\Omega_{\text{L}}^{\text{D}})$ (cf table 1) as well as the origin of the long spin coherence times: rapid momentum scattering τ_{p} due to the constant DQD confinement potential.

The measured thickness dependence of τ_{s} for electrons confined by DQDs is, however, quite different than that expected for free electrons in a undoped GaAs QWs. In the absence of lateral confinement, the spin dephasing will have a similar $[\Omega_{\text{L}}^{\text{D}}(k_{\text{F}})]^{-2}$ term associated with the vertical confinement. The momentum scattering term τ_{p}, on the other hand, is not dictated by scattering from the lateral confinement potential imposed by the DQDs, but rather by the carrier mobility. In particular, the electron mobility in GaAs QWs has been shown to vary as $(d_{\text{QW}})^n$, with $n \sim 6$, because of interface roughness scattering [31, 32], thus leading to $\tau_{\text{p}} \sim \mu \sim (d_{\text{QW}})^n$. Due to the strong dependence of τ_{p} on QW width, the spin relaxation time is expected to decrease with increasing d_{QW}, in contrast with the experimental results for spin transport via DQDs. This demonstrates, in conjunction with the very long coherence times observed in figure 2 that the spin–orbit effects on coherence cannot be attributed to simple QW effects but rather the importance of the confinement potential created by the DQDs.

4. Conclusions

In conclusion, we have shown that the precession frequency, the spin–orbit length and the spin coherence time can be controlled by the QW width. More importantly, we have demonstrated that the enhanced coherence of electron spins results from the mesoscopic confinement of the DQDs during transport, which does indeed parallel the behaviour observed in stationary quantum dots. Considering this work along with previous results showing single electron transport, mobile potentials generated by acoustic fields are thus anticipated to be a powerful and unique tool in the transport and manipulation of single quantum states in quantum information processing as well as spintronic applications.

Acknowledgments

We thank J Rudolph and K-J Friedland for comments and for a critical reading of the manuscript, and W Seidel, S Krauß and M Höricke for their technical support regarding the sample fabrication and preparation. We also acknowledge the Nanoquit consortium (BMBF, Germany). JS thanks NSERC Canada for financial support.

References

[1] D'yakonov M I and Perel' V I 1972 Spin relaxation of conduction electrons in noncentrosymmetric semiconductors *Sov. Phys. Solid State* **13** 3023–6
[2] Kiselev A A and Kim K W 2000 Progressive suppression of spin relaxation in two-dimensional channels of finite width *Phys. Rev.* B **61** 13115–20
[3] Kikkawa J M and Awschalom D D 1998 Resonant spin amplification in n-type GaAs *Phys. Rev. Lett.* **80** 4313–6
[4] Stotz J A H, Hey R, Santos P V and Ploog K H 2005 Coherent spin transport through dynamic quantum dots *Nat. Mater.* **4** 585–8
[5] Srinivas V, Chen Y J and Wood C E C 1993 Spin relaxation of two-dimensional electrons in GaAs quantum wells *Phys. Rev.* B **47** 10907–10
[6] Sandhu J S, Heberle A P, Baumberg J J and Cleaver J R A 2001 Gateable suppression of spin relaxation in semiconductors *Phys. Rev. Lett.* **86** 2150–3
[7] Mal'shukov A G, Chao K A and Willander M 1996 Quantum localization effects on spin transport in semiconductor quantum wells with zinc-blende crystal structure *Phys. Rev. Lett.* **76** 3794–7
[8] Zumbühl D M, Miller J B, Marcus C M, Campman K and Gossard A C 2002 Spin–orbit coupling, antilocalization, and parallel magnetic fields in quantum dots *Phys. Rev. Lett.* **89** 276803
[9] Zaitsev O, Frustaglia D and Richter K 2005 Role of orbital dynamics in spin relaxation and weak antilocalization in quantum dots *Phys. Rev. Lett.* **94** 026809
[10] Zumbühl D M 2004 Coherence and spin in GaAs quantum dots *PhD Thesis* Harvard University
[11] Chang C-H, Mal'shukov A G and Chao K A 2004 Spin relaxation dynamics of quasiclassical electrons in ballistic quantum dots with strong spin–orbit coupling *Phys. Rev.* B **70** 245309
[12] Holleitner A W, Sih V, Myers R C, Gossard A C and Awschalom D D 2006 Suppression of spin relaxation in submicron InGaAs wires *Phys. Rev. Lett.* **97** 036805
[13] Talyanskii V I, Shilton J M, Pepper M, Smith C G, Ford C J B, Linfield E H, Ritchie D A and Jones G A C 1997 Single-electron transport in a one-dimensional channel by high-frequency surface acoustic waves *Phys. Rev.* B **56** 15180
[14] Barnes C H W, Shilton J M and Robinson A M 2000 Quantum computation using electrons trapped by surface acoustic waves *Phys. Rev.* B **62** 8410–9
[15] Gumbs G and Abranyos Y 2004 Quantum entanglement for acoustic spintronics *Phys. Rev.* A **70** 050302
[16] Alsina F, Stotz J A H, Hey R and Santos P V 2004 Acoustically induced potential dots on GaAs quantum wells *Solid State Commun.* **129** 453–7
[17] Stotz J A H, Alsina F, Hey R and Santos P V 2005 Acoustically induced dynamic potential dots *Physica* E **26** 67–71
[18] Stotz J A H, Hey R and Santos P V 2006 Temperature dependence of spin transport by dynamic quantum dots *Mater. Sci. Eng.* B **126** 164–7
[19] Bir G L, Aronov A G and Pikus G E 1975 Spin relaxation of electrons due to scattering by holes *Sov. Phys.—JETP* **42** 705–12
[20] Sogawa T, Santos P V, Zhang S K, Eshlaghi S, Wieck A D and Ploog K H 2001 Transport and lifetime enhancement of photoexcited spins in GaAs by surface acoustic waves *Phys. Rev. Lett.* **87** 276601

[21] Baylac B, Amand T, Marie X, Dareys B, Brousseau M, Bacquet G and Thierry-Mieg V 1995 Hole spin relaxation in *n*-modulation doped quantum wells *Solid State Commun.* **93** 57–60
[22] Dresselhaus G 1955 Spin–orbit coupling effects in zinc blende structures *Phys. Rev.* **100** 580–6
[23] Stotz J A H, Hey R, Santos P V and Ploog K H 2006 Spin transport and manipulation by mobile potential dots in GaAs quantum wells *Physica* E **32** 446–9
[24] Eppenga R and Schuurmans M F H 1988 Effect of bulk inversion asymmetry on [001], [110], and [111] GaAs/AlAs quantum wells *Phys. Rev.* B **37** 10923–6
[25] Bychkov Yu A and Rashba E I 1984 Properties of a 2d electron gas with lifted spectral degeneracy *JETP Lett.* **39** 78–81
[26] Dzhioev R I, Kavokin K V, Korenev V L, Lazarev M V, Meltser Ya B, Stepanova M N, Zakharchenya B P, Gammon D and Katzer D S 2002 Low-temperature spin relaxation in n-type GaAs *Phys. Rev. B* **66** 245204
[27] Leyland W J H, John G H, Harley R T, Glazov M M, Ivchenko E L, Ritchie D A, Farrer I, Shields A J and Henini M 2007 Enhanced spin relaxation time due to electron–electron scattering in semiconductor quantum wells *Phys. Rev.* B **75** 165309
[28] Koop E J, van Wees B J and van der Wal C H 2008 Confinement-enhanced spin relaxation for electron ensembles in large quantum dots arXiv:0804.2968 [cond-mat]
[29] Beck M, Metzner C, Malzer S and Döhler G H 2006 Spin lifetimes and strain-controlled spin precession of drifting electrons in GaAs *Europhys. Lett.* **75** 597–603
[30] Crooker S A and Smith D L 2005 Imaging spin flows in semiconductors subject to electric, magnetic, and strain fields *Phys. Rev. Lett.* **94** 236601
[31] Sakaki H, Noda T, Hirakawa K, Tanaka M and Matsusue T 1987 Interface roughness scattering in GaAs/AlAs quantum wells *Appl. Phys. Lett.* **51** 1934–6
[32] Vörös Z, Balili R, Snoke D W, Pfeiffer L and West K 2005 Long-distance diffusion of excitons in double quantum well structures *Phys. Rev. Lett.* **94** 226401